Proceedings of the 11th Brazilian Congress of Thermal Sciences and Engineering -- ENCIT 2006
Braz. Soc. of Mechanical Sciences and Engineering -- ABCM, Curitiba, Brazil, Dec. 5-8, 2006

Paper CIT06-0913

H_2O_2/Paraffin Hybrid Rockets for Launching Nanosats into LEO

Leonardo Henrique Gouvêa
leo@lcp.inpe.br

Ricardo Vieira
rvieira@lcp.inpe.br

Fernando de Souza Costa
Instituto Nacional de Pesquisas Espaciais
Rodovia Presidente Dutra, km 40, Cachoeira Paulista/SP, Brasil
fernando@lcp.inpe.br

Abstract. *The launching of small payloads or nanosats into low Earth orbit (LEO) by hybrid rockets has been considered in the last years. In the present work it is determined the mass distribution of hybrid propulsion systems using H_2O_2 and solid paraffin as propellants, to place a 20 kg payload into a 300 km circular equatorial orbit. Two cases are considered: a three-stage hybrid rocket with a total characteristic velocity of 9300 m/s, and three stage air-launched rockets with a total characteristic velocity of 8700 m/s. The effects of the O/F ratio, H_2O_2 concentration and paraffin composition on specific impulse, thrust coefficient and mass distribution are studied.*

Keywords: Paraffin, H_2O_2, nanosats, low Earth orbit (LEO), specific impulse, mass distribution

1. Introduction

Hybrid rocket technology is known for more than 50 years, however only in the 1960's its safety characteristics motivated a significant research. Nowadays, the need for green propellants (propellants with low toxicity and low pollutant characteristics), the requirements of safe operation and storability, low cost missions, and the interest for launching small payloads and nanosats into LEO made hybrid rockets more attractive.

Hybrid propulsion systems employ propellants in different phases, being the most usual hybrid systems with a solid fuel and a liquid oxidizer.

The main disadvantage of hybrid rockets is the low thrust level attainable, due to the relatively low regression rates of the solid fuel grain, making necessary the use of a large number of ports. According to Karabeyoglu et al. (2003a) multi-port grains have characteristics such as:

- Large fractions of the fuel remain unburned and are not used for propulsion;
- Problems of grain integrity at the end of burning when the web thickness is too small and makes the grain susceptible to structural failure (To solve the problem, supports can be used, however they increase the mass and the complexity of the system);
- Manufacturing of multi-port grains is more difficult and expensive than of a single port grain;
- Need of multiple injectors or a pre-combustion chamber;
- Potential non-uniform burning among the ports.

Some methods to increase the fuel regression rate are known but, in general, they have undesirable characteristics, for example:

- Insert screens or mechanical devices in the ports to increase the turbulence level and, therefore, increase the heat transfer rates: this method increases the complexity of design and the failure possibilities;
- Use of metallic addictives: this method increases slightly the regression rate, however it increases the vulnerability to instabilities due to the pressure-dependence of the regression rates, and it increases the environmental impact.
- Use of oxidizers mixed within the solid fuel: this method converts the hybrid system in almost a solid system, eliminating the safety characteristics of the hybrid system;
- Increase the surface rugosity adding small solid particles, which would burn at a different rate from the main fuel: this method has a small effect on regression rates but large solid particles in the exhaust gases reduce the system efficiency, and it causes an increase in costs of fuel production.

The safe operation of hybrid propulsion systems is related to the separation of fuel and oxidizer, differently from solid systems which mix fuel and oxidizer in the grain. Another important safety characteristic is the independence of the regression rate with respect to the chamber pressure, making hybrid systems safer than solid systems if pressure peaks do occur.

The control of the oxidizer flow rate in hybrid systems allows several starts and an accurate control of the thrust level.

Hybrid systems have only one liquid propelllant, thus they require only one liquid line and a relatively simple injection system, as compared to liquid bipropellant systems which require two separate liquid lines and a complex injection plate in order to collide and mix the fuel and oxidizer jets.

The hydrogen peroxide (H_2O_2) is a well-known oxidizer or monopropellant and has been used for decades in propulsion systems, as described by Walter (1954), who related his experiences with the German Navy during the II World War, when hydrogen peroxide was used in ATO (Assisted Take Off) engines. He describes the decomposition and detonation characteristics of peroxide and mentions that peroxide at concentrations lower than 82 % is not detonable and that pressure does not affect the peroxide decomposition velocity. Williams et al. (2004) states that HTP (High Teste Peroxide) is similar to nitroglicerin in terms of shock sensitivity and explodes with the same strength than the same quantity of TNT (Trinitrotoluen).

The paraffin used as fuel, specially in candles, is part of human culture for hundreds of years, but only in the last 5-10 years, has beeen considered as a rocket fuel.

Recently, it was developed in the Stanford University and in the Ames-NASA Research Center, both in the USA, a new paraffin-based fuel whose regression rate is approximately three times higher than conventional hybrid fuels (Karabeyoglu et al., 2003a,b, 2004). Promising results were obtained by several researchers (Brown and Lydon, 2005; Karabeyoglu et al., 2004; Santos et al., 2005; McCormick et al., 2005) using paraffin with different oxidizers – liquid oxygen (LOX), gaseous oxygen (GOX), nitrous oxide (N_2O) and hydrogen peroxide (H_2O_2).

Figure 1 shows the regression rates of paraffin with different oxidizers, for various oxidizer flow rates.

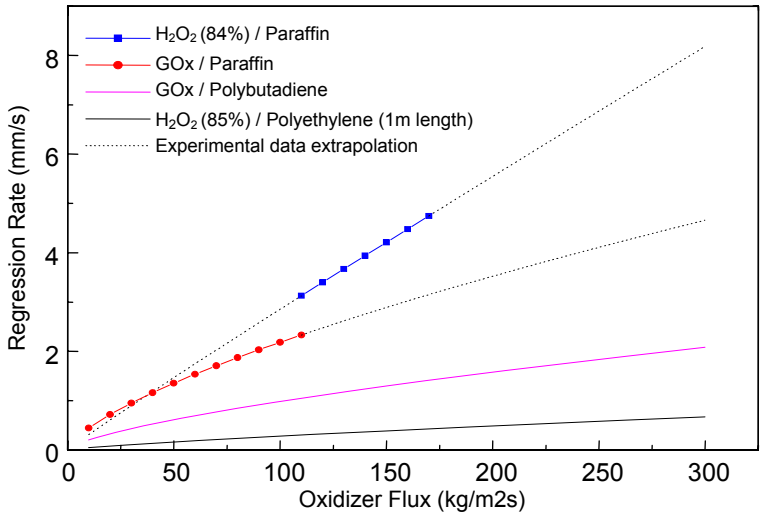

Figure 1. Regression rate of paraffin burning with different oxidizers versus oxidizer flow rates.

The mass of the propulsion systems can be significantly reduced by using air launching rockets, since there is lower drag, lower gravitational losses, and there is a gain in the system initial velocity.

The objective of this work is to describe hybrid propulsion systems using paraffin/H_2O_2 to launch a 20 kg nanosat into a low Earth equatorial circular orbit of 300 km. Two cases are considered: i) a three stage rocket with a total characteristic velocity of 9300 m/s; and ii) a three stage air-launched rocket with a total characteristic velocity of 8700 m/s.

2. Propulsion Performance Parameters

The efficiency parameters of a propulsion system depend on the combustion characteristics. The reaction between paraffin and hydrogen peroxide in the rocket combustion chamber is described by the chemical equation:

$$C_n H_{2n+2} + \left(\frac{3n+1}{\phi x}\right)\left(xH_2O_2 + (1-x)H_2O\right) \rightarrow \eta_{H_2O}H_2O + \eta_{CO_2}CO_2 + \eta_{CO}CO + \eta_{H_2}H_2 + \eta_{O_2}O_2 + \eta_{OH}OH + \eta_O O + \eta_H H \quad (1)$$

where x is the molar fraction of peroxide in the solution, ϕ is the fuel/oxidizer equivalence ratio and η_i is the stoichiometric coefficients of product i. A chemical equilibrium code was written in MATLAB language, using the equilibrium constant method, to calculate the stoichiometric coefficients in Eq. (1) and the adiabatic flame temperature, T_c. From these data, obtained with a given chamber pressure, P_c, the following variables are calculated:

$$X_j = \eta_j \big/ \eta_{total} \tag{2}$$

$$M_{prod} = \sum_{j=1}^{N} \eta_j X_j \tag{3}$$

$$\bar{C}_p = \sum_{j=1}^{N} X_j \bar{C}_{p,j} \tag{4}$$

$$\gamma = \bar{C}_p \big/ \left(\bar{C}_p - \bar{R} \right) \tag{5}$$

where X_j is the molar fraction of each product species, M_{prod} is the molar mass of products, $\bar{C}_p$ is the molar specific heat at constant pressure, γ is the ratio of specific heats, $\bar{R} = R_o/M_{prod}$ is the gas constant, and R_o = 8314 kJ/kmolK is the universal gas constant. The specific heats are temperature functions obtained from NIST (www.nist.gov).

After calculation of the chamber conditions, i.e., M_{prod}, γ and T_c, at a given chamber pressure, P_c, several propulsion performance parameters can be calculated: specific impulse, *Isp*; exhaustion characteristic velocity, C*; thrust coefficient, C_F; the mass flow rate, $\dot{m}$; and thrust, F, for a given ambient pressure, P_a, and nozzle expansion rate, ε.

The propulsion parameters are calculated with the following simplifying assumptions:

- Isentropic flow in the chamber and nozzle;
- Frozen flow along the nozzle;
- Constant pressure in the chamber;
- Perfect gases and perfect mixture;.
- Average γ in the nozzle.

The specific impulse, for a constant thrust rocket, is defined as the ratio between thrust and weight consumption rate of propellants:

$$I_{sp} = C_F C^* \big/ g_0 \tag{6}$$

where g_0 is the gravity acceleration at sea-level.

The characteristic exhaustion velocity C^* is given by

$$C^* = \sqrt{\gamma R T_c} \big/ \Gamma \tag{7}$$

where $\Gamma = \gamma \left[2 \big/ (\gamma + 1) \right]^{\frac{\gamma+1}{2(\gamma-1)}}$.

The thrust coefficient, C_F, is given by:

$$C_F = \sqrt{\left(\frac{2\gamma^2}{\gamma - 1} \right) \left(\frac{2}{\gamma + 1} \right)^{(\gamma+1)/(\gamma-1)} \left[1 - \left(\frac{P_e}{P_c} \right)^{(\gamma-1)/\gamma} \right]} + \frac{P_e - P_a}{P_c} \frac{A_e}{A_t} \tag{8}$$

where A_e is the nozzle exit area, A_t is the nozzle throat area and P_e is the nozzle exit pressure. The thrust F generated by the exhaustion of gases through the nozzle is calculated by

$$F = \dot{m} v_e + \left(P_e - P_a \right) A_e \tag{9}$$

where $\dot{m}$ is the propellants mass flow rate, given by

$$\dot{m} = \Gamma \frac{A_t P_c}{\sqrt{\gamma R T_c}} \tag{10}$$

and v_e is the products exhaustion velocity, given by

$$v_e = \sqrt{\frac{2\gamma RT_c}{\gamma - 1}\left[1 - \left(\frac{P_e}{P_c}\right)^{\frac{(\gamma-1)}{\gamma}}\right]} \tag{11}$$

Equation (8) shows that the thrust coefficient is function of γ that depends on temperature and products composition. Figure 2 shows the effects of the H_2O_2 mass fraction and O/F (oxidizer/fuel) mass ratio on thrust coefficient, assuming γ frozen at chamber conditions and assuming an average γ along the nozzle. As can be seen in Fig. 2 there is a small difference of about 0.7 % in C_F values for the two cases.

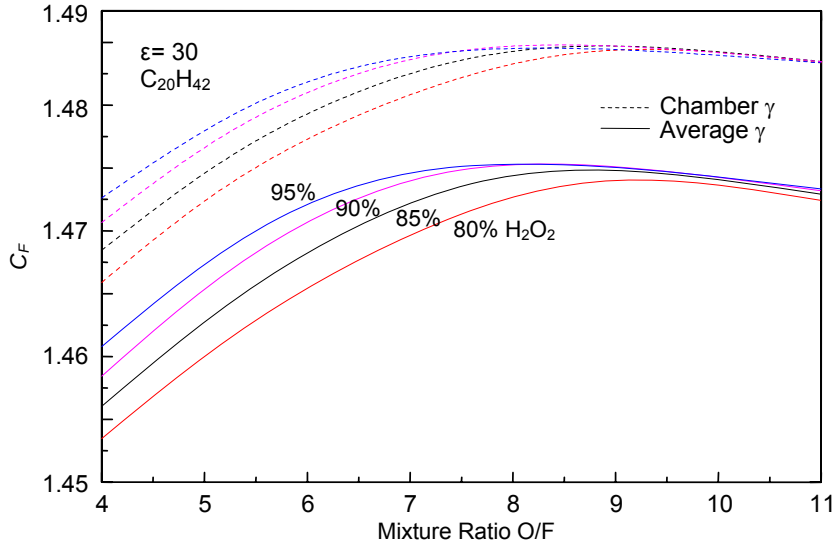

Figure 2. Effects of O/F mass mixture ratio and hydrogen peroxide mass fraction on thrust coefficient, C_F.

Figures 3 and 4 show the effects of hydrogen peroxide mass fraction and O/F mass ratio on specific impulse and on adiabatic flame temperature, respectively, for different paraffin fuels. It can be verified in Figs. 3 and 4 that both specific impulse and combustion temperature increase with increasing hydrogen peroxide mass fractions, since the reduction in water content increases the products temperature.

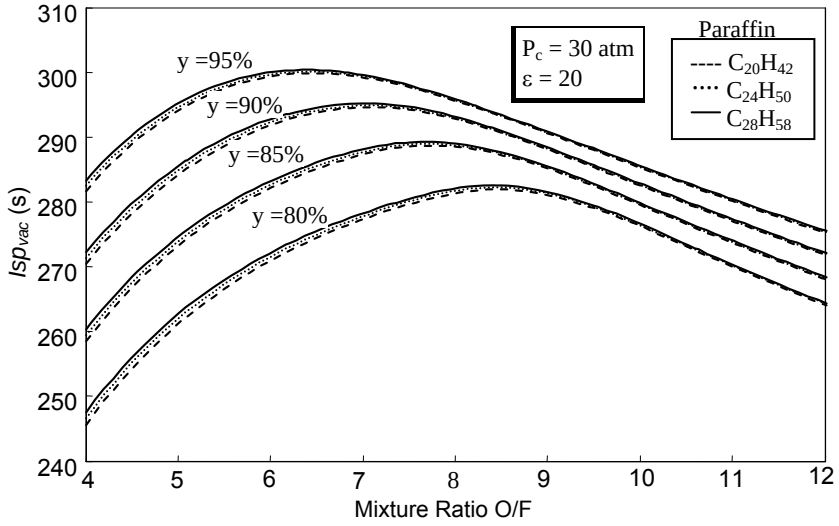

Figure 3. Effects of O/F mass mixture ratio and hydrogen peroxide mass fraction on specific impulse, for different paraffin fuels.

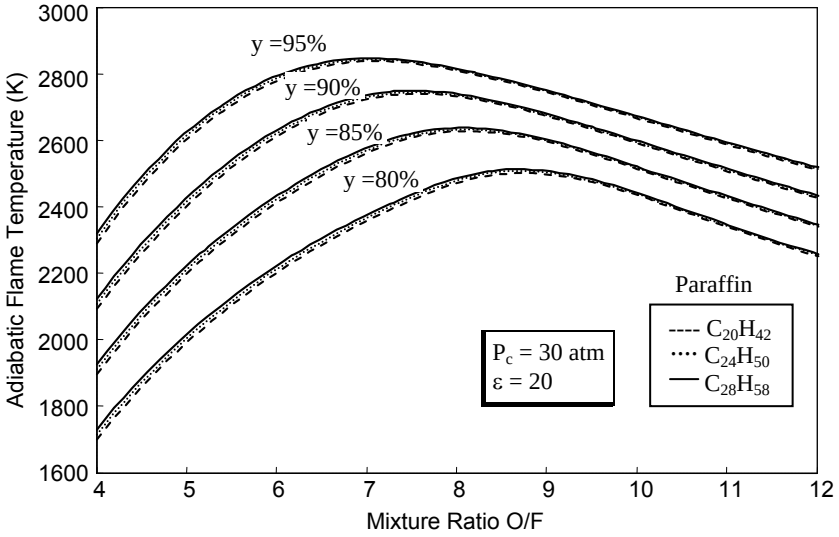

Figure 4. Effects of O/F mass mixture ratio and hydrogen peroxide mass fraction on combustion temperatures, for different paraffin fuels.

It can be verified on Fig. 3 that there is a reduction on the ideal O/F mass ratio, which yields the largest specific impulses, from 8.5 to 6.4 when the peroxide mass fraction increases from 80 to 95 %. The required mass of oxidizer per unit mass of paraffin decreases with increasing peroxide concentrations.

The paraffin molecular size has negligible effect on specific impulses and adiabatic flame temperatures, as shown in Figs. 3 and 4.

Karabeyoglu et al. (2003) studied the effects of adding aluminum particles to solid paraffin. They found that an aluminum content of 40% in mass can increase up to 25% the regression rate of paraffin burning with N_2O.

Therefore, the NASA CEA-2004 equilibrium code was used to study the influence of Al mass fraction of paraffin burning with H_2O_2 on specific impulses and adiabatic flame temperatures, as shown by Figs. 5 and 6, respectively.

It was observed a significant increase of maximum specific impulses assuming equilibrium flow along the nozzle, but no significant effects on maximum specific impulses assuming frozen flow along the nozzle. The most important effect in both cases – with equilibrium or frozen nozzle flows - was a continuous reduction of the ideal O/F mixture ratios with Al content, thus allowing a potential reduction on oxidizer mass. As seen in Fig. 6, the maximum flame temperature increases and its corresponding O/F ratio diminishes with Al mass fraction.

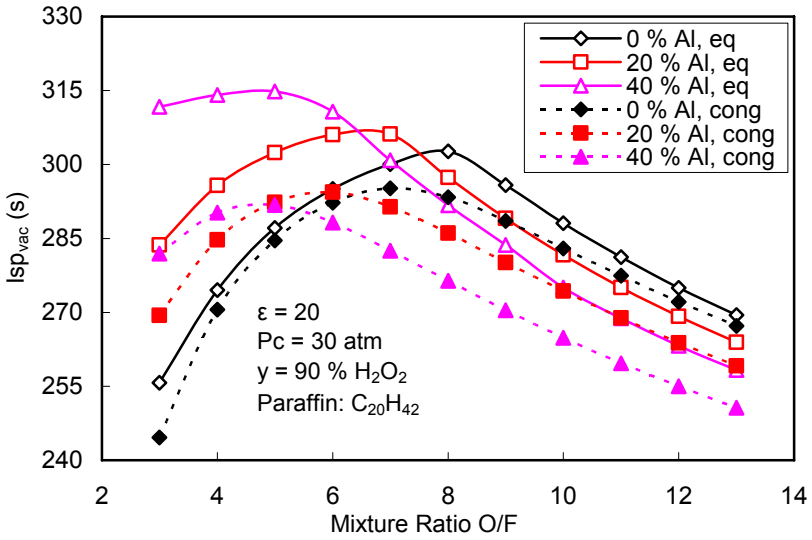

Figure 5. Effects of O/F mass mixture ratio and Al mass fraction in paraffin on vacuum *Isp*, considering equilibrium and frozen nozzle flows.

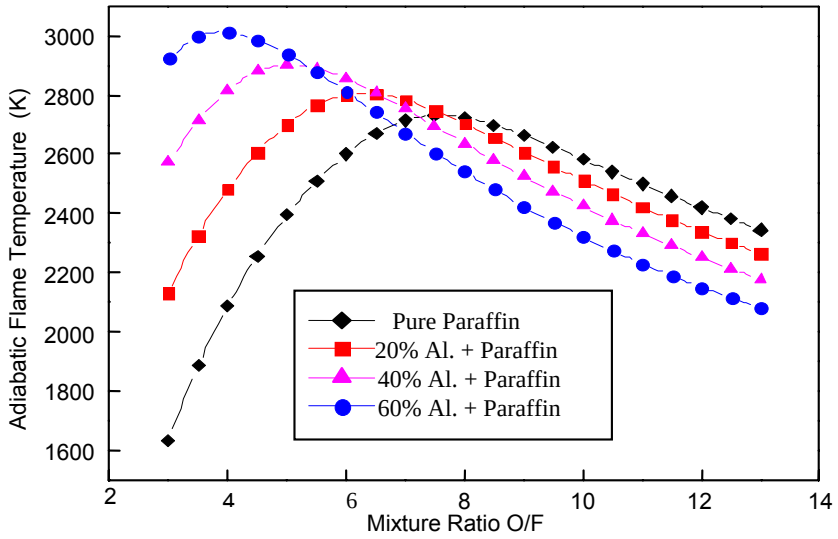

Figure 6. Effects of O/F mass mixture ratio and Al mass fraction in paraffin on adiabatic flame temperature, T_c, considering a frozen nozzle flow. Propellants: $C_{20}H_{42}$ burning with 90% H_2O_2.

In order to compare the performance of paraffin with other common hybrid fuels (PE and HTPB) and a common liquid fuel (RP-1 querosene), their specific impulses were calculated using 90% H_2O_2 as oxidizer, as depicted in Fig. 7. It can be seen in Fig. 7 that all fuels present similar specific impulses. However, since paraffin presents higher regression rates than HTPB and PE, it can yield a larger thrust for a given propulsion system configuration, and the bipropellant system RP-1/H_2O_2 is more complex and expensive.

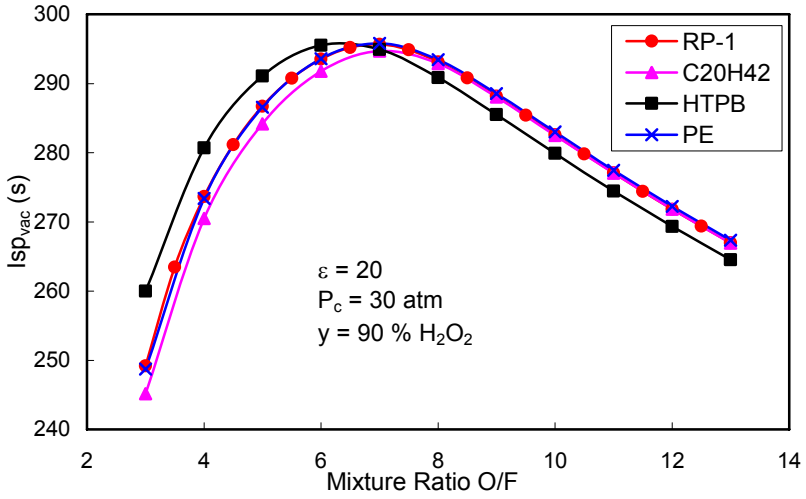

Figure 7. Effects of O/F mass mixture ratio on specific impulses of several propellants burning with 90% H_2O_2.

3. Rocket Mass Distribution

In this section it is presented a preliminary analysis of the mass distribution of rockets to place a nanosat of 20 kg into a circular equatorial LEO of 300 km, using paraffin and H_2O_2 as propellants. Two configurations are analysed and compared: a three stage rocket launched from ground and a three stage air-launched rocket. The characteristic velocities for these two rockets are given next.

A circular low Earth orbit velocity, v_{LEO}, of a rocket can be calculated by integration of the 2nd Newton law applied to the rocket, which can be written as:

$$v_{LEO} = \int_{t_0}^{t_f} \frac{F}{m} dt - \int_{t_0}^{t_f} \frac{F}{m}(1-\cos\alpha)\, dt - \int_{t_0}^{t_f} \frac{D}{m} dt - \int_{t_0}^{t_f} g \sin\gamma dt \qquad (12)$$

where D is drag, F is thrust, m is the instantaneous rocket mass, α is the steering angle or angle between the thrust vector and the velocity vector, γ is the local flight path angle or angle from local horizontal to velocity vector, t is time, t_o is the ignition time and t_f is the burnout time. Defining:

Mission characteristic velocity: $$\Delta V = \int_{t_0}^{t_f} \frac{F}{m} dt \tag{13a}$$

Steering characteristic velocity: $$\Delta V_{steering} = \int_{t_0}^{t_f} \frac{F}{m}\left(1-\cos\alpha\right) dt \tag{13b}$$

Drag characteristic velocity: $$\Delta V_{drag} = \int_{t_0}^{t_f} \frac{D}{m} dt \tag{13c}$$

Gravitational characteristic velocity: $$\Delta V_{gravitational} = \int_{t_0}^{t_f} g \sin\gamma dt \tag{13d}$$

The mission characteristic velocity can be calculated by

$$\Delta V = v_{LEO} + \Delta V_{steering} + \Delta V_{drag} + \Delta V_{gravitational} \tag{14}$$

The LEO circular velocity at 300 km height is obtained from:

$$v_{LEO} = \sqrt{\frac{M_{Earth} G}{R_{Earth} + h}} = \sqrt{\frac{5.9742\times10^{24}\times6.6742\times10^{-11}}{6378+300}} = 7714 m/s \tag{15}$$

Humble et al. (1995) presents historical data of steering, drag and gravitational characteristic velocities for LEO missions, yielding mission characteristic velocities from 8800 to 9300 m/s. In this work it is considered ΔV = 9300 m/s for a ground-launched rocket and ΔV = 8700 m/s for air-launched rockets. For comparison, the well-known Pegasus rocket is launched by an airplane with M = 0.8 at 10 km height, yielding an initial velocity of 243 m/s, and lower drag, steering and gravitational losses than ground launched rockets.

The inert mass fraction, f_{inert}, and the propellant mass fraction, f_{prop}, of a stage are defined, respectively, by:

$$f_{inert} = \frac{m_{inert}}{m_{prop} + m_{inert}} \tag{16}$$

$$f_{prop} = 1 - f_{inert} \tag{17}$$

where m_{inert} is the stage mass excluding the payload mass and m_{prop} is the stage propellant mass. It should be noted that the payload mass of a given stage is the added mass of all upper stages.

Tables 1 and 2 show the inert mass fractions and the propellant mass fractions of several solid and liquid propellant rocket engines. The inert mass fractions depicted on Tables 1 and 2 vary from 0.07 to 0.19 for liquid rocket motors, and from 0.061 to 0.141 for solid rocket motors.

Tables 3 and 4 show the initial conditions assumed for the preliminary design of a 20 kg nanosat hybrid launcher, considering a three stage ground launched rocket and a three stage air launched rocket.

The parameter F/W_0 on Tables 3 and 4 is the ratio between stage thrust, F, and the initial stage weight, W_0, expressed in terms of g number. The F/W_0 and nozzle expansion rates were obtained from historical data (Isakowitz et al., 1999).

For the rocket systems analysed in this paper, it was adopted a conservative value f_{inert} = 0.15, based on data from Tables 1 and 2, F/W_0 = 2.5 and a chamber pressure P_c = 3 MPa for each stage.

Thrust and specific impulses of each stage were considered constants for the preliminary design and the O/F ratios were chosen to yield the maximum Isp's for pure paraffin reacting with 90 % H_2O_2.

Table 1. Mass distributions and fractions of Solid Rocket Motors (adapted from Humble et al., 1995)

Motor Designation	**Propellant**	**Insulation**	**Case**	**Nozzle**	**Igniter**	**Misc.**	**Inert**	f_{prop}	f_{inert}
Castor IVA	10,101	234	749	225	10	276	1494	0.871	0.129
GEM	11,767	312	372	242	7.9	291	1224.9	0.906	0.094
ORBUS 21	9707	145	354	143	16	7	665	0.936	0.064
OBUS 6E	2721	64.1	90.9	105.2	9.5	5.3	275	0.908	0.092
Star 48B	2010	27.1	58.3	43.8	0.0	2.2	131.4	0.939	0.061
Star 37XFP	884	12.7	26.3	31.7	0.0	1.3	72	0.915	0.085
Star 63D	3250	71.4	106.3	60.8	1.0	11.6	251.1	0.928	0.072
Orion 50SAL	12,160	265.2	547.9	235.4	9.1	21.0	1078.6	0.918	0.082
Orion 50	3024	75.6	133.4	118.7	5.3	9.9	342.9	0.898	0.102
Orion 38	770.7	21.9	39.4	52.8	1.3	10.6	126	0.859	0.141

Table 2. Mass distributions and fractions of Liquid Rocket Motors (adapted from Isakowitz et al., 1999)

Motor Designation	**Propellant**	**Inert**	f_{prop}	f_{inert}
YF-40	14,200	1,000	0.93	0.07
YF-73	8,500	2,000	0.81	0.19
11D49	18,700	1,435	0.93	0.07
LE5-A	14,000	2,700	0.84	0.16
LE-5B	16,600	3,000	0.85	0.15
RL10B-2	16,820	2,457	0.87	0.13
AJ10-118K	6,004	950	0.86	0.14
RS27A	95,500	6,820	0.93	0.07
11D58M	14,600	2,720	0.84	0.16
RD-171	325,700	28,600	0.92	0.08

Table 3. Initial conditions for preliminary design of a three stage ground-launched hybrid rocket.

ΔV_{total} (m/s)	9300		
STAGES	**1**	**2**	**3**
ΔV_j, j = 1, 2, 3 (m/s)	3100	3100	3100
Expansion rate, ε (-)	10	40	60
Isp (s)	262	291	297

Table 4. Initial conditions for preliminary design of a three stage air-launched hybrid rocket.

ΔV_{total} (m/s)	8700		
STAGES	**1**	**2**	**3**
ΔV_j, j = 1, 2, 3 (m/s)	2900	2900	2900
Expansion rate, ε (-)	10	40	60
Isp (s)	262	291	297

3.1 Masses, Consumption Rates and Burning Times

The j-stage propellant mass is given by

$$m_{prop,j} = \frac{m_{pay,j}\left[e^{\left(\Delta V_j / Isp_j g_0\right)} - 1\right]}{1 - f_{inert} e^{\left(\Delta V_j / Isp_j g_0\right)}} \tag{18}$$

where $m_{pay,j}$ is the j-stage payload, which is the initial mass of the j+1-stage.

The j-stage inert mass is calculated from

$$m_{inert,j} = \frac{f_{inert,j}}{1 - f_{inert,j}} \tag{19}$$

The *j*-stage initial mass is given by

$$m_{0,j} = m_{prop,j} + m_{inert,j} + m_{pay,j} \tag{20}$$

The *j*-stage average thrust (assumed as constant) is obtained from

$$F_j = \left(F/W_0\right)_j m_{0,j} g_0 \tag{21}$$

The *j*-stage propellant consumption rate, $\dot{m}_{prop,j}$, is obtained from

$$\dot{m}_{prop,j} = F_j \Big/ \left(Isp_j g_0\right) \tag{22}$$

The *j*-stage fuel consumption rate, $\dot{m}_{fuel,j}$, is

$$\dot{m}_{fuel,j} = \frac{\dot{m}_{prop,j}}{1 + \left(O/F\right)_j} \tag{23}$$

The *j*-stage oxidizer consumption rate, $\dot{m}_{oxid,j}$, is

$$\dot{m}_{oxid,j} = \dot{m}_{prop,j} \frac{\left(O/F\right)_j}{1 + \left(O/F\right)_j} = \dot{m}_{prop,j} - \dot{m}_{fuel,j} \tag{24}$$

The burning time, t_b, is obtained from

$$t_{b,j} = \frac{m_{prop,j}}{\dot{m}_{prop,j}} \tag{25}$$

Tables 5 and 6 show the masses and burn times using Eqs. (18-25) with the initial conditions presented on Tables 3 and 4, for three stage ground-launched rockets and three stage air-launched rockets, respectively.

Table 5. Results for a three stage ground launched rocket.

STAGE		**1**	**2**	**3**
m_{prop}	(kg)	1574.5	261.6	57
m_{fuel}	(kg)	196.8	32.7	7.1
m_{oxid}	(kg)	1377.7	228.9	49.9
m_{pay}	(kg)	394.9	87.14	**20**
m_{inert}	(kg)	277.9	46.16	10
$\dot{m}_{prop}$	(kg/s)	21.4	3.39	0.73
$\dot{m}_{fuel}$	(kg/s)	2.6	0.42	0.09
$\dot{m}_{oxi}$	(kg/s)	18.8	2.97	0.64
t_b	(s)	73.4	77.1	77.8
m_0	(kg)	**2247**	394.9	87.14

Table 6. Results for a three stage air launched rocket.

STAGE		**1**	**2**	**3**
m_{prop}	(kg)	1027.7	197.9	48.8
m_{fuel}	(kg)	128.5	24.7	6.1
m_{oxid}	(kg)	899.2	173.2	42.7
m_{pay}	(kg)	310.3	77.4	**20**
m_{inert}	(kg)	181.3	34.9	8.61
$\dot{m}_{prop}$	(kg/s)	14.5	2.6	0.65
$\dot{m}_{fuel}$	(kg/s)	1.82	0.3	0.08
$\dot{m}_{oxi}$	(kg/s)	12.68	2.3	0.57
t_b	(s)	70.9	74.3	74.9
m_0	(kg)	**1519**	310.3	77.4

Figure 8 shows the variation of the stage total mass versus f_{inert} for the two cases considered. It can be noted that the stage total mass grows exponentially with f_{inert}, i.e., a small variation on f_{inert} causes significant changes on the total vehicle mass.

If the payload mass - with upper stages' masses - is included as inert mass of a given stage, the inert mass fractions of all stages become about 0.3 and higher.

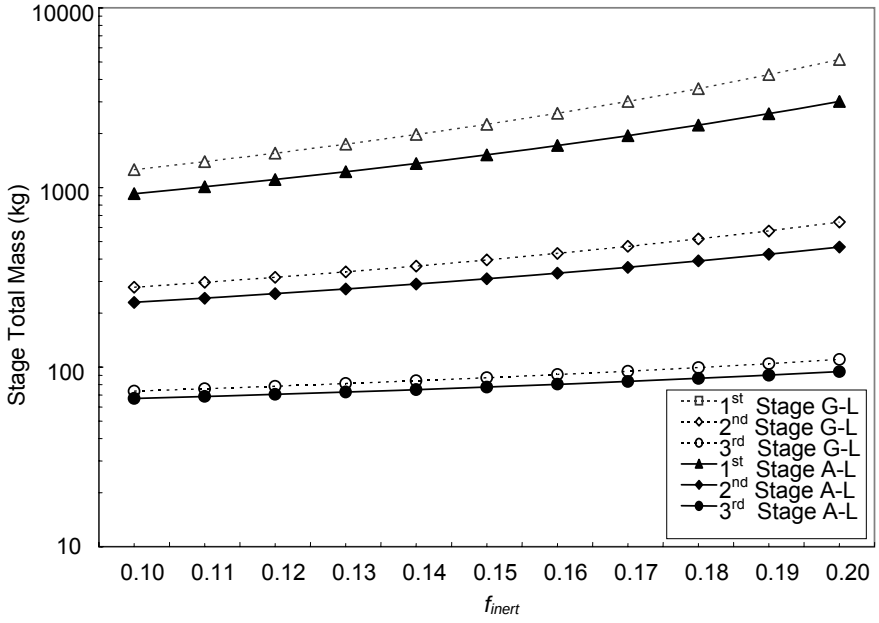

Figure 8. Effects of inert mass fraction on the stages' total mass for three stage ground-launched rockets (G-L) and three stage air-launched rockets (A-L)

5. Comparison of Results and Conclusions

This paper presented a preliminary analysis of the mass distribution of rockets to place a nanosat of 20 kg into a circular equatorial LEO of 300 km, using paraffin and H_2O_2 as propellants.

It was verified that paraffin has a good potential as a hybrid fuel when compared to other polymers and RP-1, using hydrogen peroxide as oxidizer. Hydrogen peroxide can be decomposed catalytically and generates O_2 and H_2O at high temperatures. Thus it is not required an ignition system to burn the fuel. It has a relatively high density (~1.4 g/cm^3) (Schumb, 1995) which reduces the tank weight and size. It can be also used as a pressurizer.

The preliminary design indicated that an air-launched three stage hybrid rocket would have a total initial mass of about 1520 kg, yielding a payload fraction of 1.316 %, while a ground-launched three stage hybrid rocket would have a total initial mass of about 2250 kg, in order to launch a 20 kg nanosat into LEO, with a payload fraction of 0.889 %.

In the analysis, an inert mass fraction of 0.15 was adopted, exclusive of the payload mass.

For comparison, Rothman and Siegenthaler (2003) designed a three-stage air launched rocket using off the shelf engines, and calculated an initial gross mass of 4550 kg for launching a 100 kg microsatellite into LEO, with a payload fraction of 2.198 %. The Brazilian VLS-1 launcher (www.aeb.gov.br) is designed for launching 300 kg into LEO with an initial mass of 50000 kg, and presents a payload fraction of 0.6 %.

It is seen that a three-stage air-launched rocket presents the lower initial mass, therefore the higher payload ratio. Air launched rockets can be launched almost anywhere, anytime and do not require a ground launching base, however they require the adaptation of an airplane for proper rocket release.

6. References

Brown, T. R., Lydon, M.C., 2005, "Testing of Paraffin-Based Hybrid Rocket Fuel Using Hydrogen Peroxide Oxidizer", AIAA Region 5 Student Conference, Wichita, USA.

CEA 2004 – "Chemical Equilibrium with Applications", Cleveland, OH: Glenn Research Center-NASA.

Humble, R. W., Altman, D., 1995, "Hybrid Rockets Propulsion Systems". Ed. Hollander, M.A, Space propulsion analysis and design., cap.7, pp. 365-370 .

Huzel, D. K., Huang, D. H., 1992, "Introduction To Liquid-Propellant Rock Engines", Washington, D. C., AIAA. cap. 1, pp. 4-17.

Isakowitz, S. J., Hopkins Jr, J. P., Hopkins, J. B., 1999, " International Reference Guide to Space Lauch Systems" Washington, D.C., American Institute of Aeronautics and Astronautics, 549 p.

Karabeyoglu, A., Zilliac, G., Cantwell, B.J., Dezilwa, S., Castellucci, P., 2003, "Scale-up Tests of High Regression Rate Liquefying Hybrid Rocket Fuels", 41st Aerospace Sciences Meeting and Exhibit. Nevada, USA.

Karabeyoglu, A., Zilliac, G., Cantwell, B.J., Dezilwa, S., Castellucci, P., 2004, "Scale-up Tests of High Regression Rate Paraffin-Based Hybrid Rocket Fuels", Journal of Propulsion and Power, v.20, n.6, pp. 1037-1045, November-December.

Karabeyoglu, A., Zilliac, G., Castellucci, P, Urbanczyk, P., Stevens, J., Inalhan, G., Cantwell, B,J., 2003, "Development of High-Burning-Rate Hybrid-Rocket-Fuel Flight Demonstrators", 39th AIAA/ASME/SAE/ASEE Joint Propulsion Conference, Huntsville, Alabama, USA.

McCormick, A., HultgreN, E., Lichtman, M., Smith, J., Sneed, R., Azimi, S. 2005, "Design, Optimization, and Launch of a 3" Diameter N_2O/Aluminized Rocket", AIAA/ASME/SAE/ASEE Joint Propulsion Conference and Exhibit, 41, Tucson, Arizona, USA.

Rothman, J., Siegenthaler, E., 2003, "The F-15 Microsatellite Launch Vehicle", 1st Responsive Space Conference, AIAA-LA Section/SSTC, April 1–3, Redondo Beach, CA, USA.

Santos, L. M. C., Almeida, L.A.R, Veras, C.A.G., 2005, "Design and Flight Test of a Paraffin Based Hybrid Rocket", 18th International Congress of Mechanical Engineering, Ouro Preto, Brasil.

Schumb, W. C.; Satterfield, C. N.; Wentworth, R. L., 1955, "Hydrogen Peroxide", New York: Reinhold Publishing Corporation, 759 p.

Sutton, G. P., 1992, "Rocket Propulsion Elements, An Introduction to the Engineering of Rockets", New York: Wiley, 636 p.

Williams, G., Macklin, F., Sarigul-Klijn, M., Sarigul-Klijn, N., Bendon, J., 2004, "Almost There: Responsive Space", 2nd Responsive Space Conference , Los Angeles, CA, USA.